

DOI:10.1002/ejic.201402740

## Three Scandium Compounds with Unsaturated Coordinative Metal Sites – Structures and Catalysis

Liying Zhang,<sup>[a]</sup> Li Wang,<sup>[a]</sup> PengCheng Wang,<sup>[a]</sup> Tianyou Song,<sup>[a]</sup>  
Da Li,<sup>[a]</sup> Xiaobo Chen,<sup>[b]</sup> Yong Fan,<sup>\*[a]</sup> and Jianing Xu<sup>\*[a]</sup>

**Keywords:** Scandium / Organic–inorganic hybrid composites / Heterogeneous catalysis / Cyanosilylation

Two scandium coordination polymers, a 2D supermolecule structure  $\{[\text{Sc}(\text{OH})(\text{L}^1)_2(\text{H}_2\text{O})]\}_n$  (**1**) ( $\text{HL}^1$  = isonicotinic acid), a 1D infinite chain structure  $\{[\text{Sc}_3(\text{L}^2)_4(\text{H}_2\text{O})_4]\cdot\text{NO}_3\cdot\text{H}_2\text{O}\}_n$  (**2**) ( $\text{H}_2\text{L}^2$  = 4,5-imidazole dicarboxylic acid), as well as a scandium complex  $\{[\text{Sc}_2(\text{OH})_2(\text{L}^3)_2(\text{H}_2\text{O})_4]\}_n$  (**3**) ( $\text{H}_2\text{L}^3$  = 1,2,3-triazole-4,5-dicarboxylic acid), were synthesized and charac-

terized by X-ray crystallography. Compounds **1–3** are active heterogeneous catalysts for high-yield cyanosilylation of aromatic aldehydes in acetonitrile, particularly for *p*-nitrobenzaldehyde. Moreover, these three catalysts can be reused three times without significant loss in activity or mass.

### Introduction

Heterogeneous catalysis is a vital component that has been exploited by about 90% of the existing chemical manufacturing processes.<sup>[1]</sup> Metal coordination polymers are emerging solid materials for heterogeneous catalysis, with regard to their high surface area, well-defined porous structure, and chemical tunability.<sup>[2]</sup> Coordination polymers can act as heterogeneous Lewis acid catalysts, because they can provide unsaturated coordinative nodes or form active metal complexes that are incorporated into the linking ligands. Moreover, metals and ligands are strongly bound within the framework, which prevents decomposition in solutions. Therefore, compared to discrete molecular containers, coordination polymers have a number of advantages, such as high thermal stability, easy crystallization in high yields, and low solubility in common solvents.<sup>[3]</sup>

Recently, scandium coordination polymers (Sc-CPs) with thermally stable frameworks have demonstrated interesting catalytic properties in green chemistry.<sup>[4]</sup> For example, a Sc-CP built from squaric acid,  $\text{Sc}_2(\text{C}_4\text{O}_4)_3$ , can act as an efficient heterogeneous catalyst both in cyanosilylation and acetalization of carbonyl compounds.<sup>[5]</sup> A new hybrid organic–inorganic polymer,  $\text{Sc}_2(\text{OOCCH}_2\text{H}_4\text{COO})_{2.5}(\text{OH})$ , prepared by Snecko and co-workers can be used as an effective Lewis acid catalyst in the Friedel–Crafts acylation reaction

and can easily be recycled and reused without any appreciable loss in activity.<sup>[6]</sup> Although the interest in Sc has been increasing recently because of the successful utilization of its compounds in organic chemistry<sup>[7]</sup> and the preparation of some polymer-supported Sc catalysts, there are only a few examples of Sc-CP-based heterogeneous catalysts showing a high stability and desirable properties.<sup>[5,8]</sup>

The cyanosilylation reaction is an important C–C bond-forming reaction that is catalyzed by Lewis acids.<sup>[9]</sup> It provides a convenient route to prepare cyanohydrins, which are key derivatives in the synthesis of fine chemicals and pharmaceuticals.<sup>[10]</sup> In coordination polymers, vacant coordination site(s) associated with the metal centers and/or functional organic sites for possible interactions with reactants have been reported to catalyze this reaction.<sup>[11]</sup> Thus we aim to design and synthesize robust Sc compounds containing coordinative unsaturated metal sites.

### Results and Discussion

Two Sc-CPs and one Sc complex,  $\{[\text{Sc}(\text{OH})(\text{L}^1)_2(\text{H}_2\text{O})]\}_n$  (**1**) ( $\text{HL}^1$  = isonicotinic acid),  $\{[\text{Sc}_3(\text{L}^2)_4(\text{H}_2\text{O})_4]\cdot\text{NO}_3\cdot\text{H}_2\text{O}\}_n$  (**2**) ( $\text{H}_2\text{L}^2$  = 4,5-imidazole dicarboxylic acid), and  $\{[\text{Sc}_2(\text{OH})_2(\text{L}^3)_2(\text{H}_2\text{O})_4]\}_n$  (**3**) ( $\text{H}_2\text{L}^3$  = 1,2,3-triazole-4,5-dicarboxylic acid), were synthesized on the basis of three different carboxylate ligands. These three new Sc compounds display good catalytic activity for the cyanosilylation of aromatic aldehydes, especially for *p*-nitrobenzaldehyde.

### Crystallographic Structure of 1

Compound **1** crystallizes in the monoclinic space group  $P2_1/c$ , and its asymmetric unit contains one  $\text{Sc}^{\text{III}}$  ion, two

[a] State Key Laboratory of Inorganic Synthesis and Preparative Chemistry, College of Chemistry, Jilin University  
Jiefang road 2519, Changchun, China  
E-mail: mrfy@jlu.edu.cn  
xujn@jlu.edu.cn

[b] Department of Materials Engineering, Monash University  
Clayton, VIC 3800, Australia

Supporting information for this article is available on the WWW under <http://dx.doi.org/10.1002/ejic.201402740>.

$L^1$  ligands, one OH group, and one coordinated water molecule (Figure S1). The 2D structure of **1** is constructed from the infinite chains  $\text{Sc}(\text{OH})(L^1)_2(\text{H}_2\text{O})$  by  $\pi\cdots\pi$  stacking interactions of  $L^1$  ligands. There are two kinds of six-coordinate  $\text{Sc}^{\text{III}}$  ions. The coordination geometry of Sc1 can be described as an octahedron with two oxygen atoms from two independent  $L^1$  ligands, two oxygen atoms from two OH groups, and two oxygen atoms from two terminal water molecules to complete the coordination sphere. The Sc2 octahedron is linked by four oxygen atoms from four independent  $L^1$  ligands and two oxygen atoms from two OH groups (Figure 1). The Sc–O bond lengths fall in the region of 2.0619(18)–2.1331(18) Å; these values are consistent with those of similar compounds.<sup>[12]</sup>

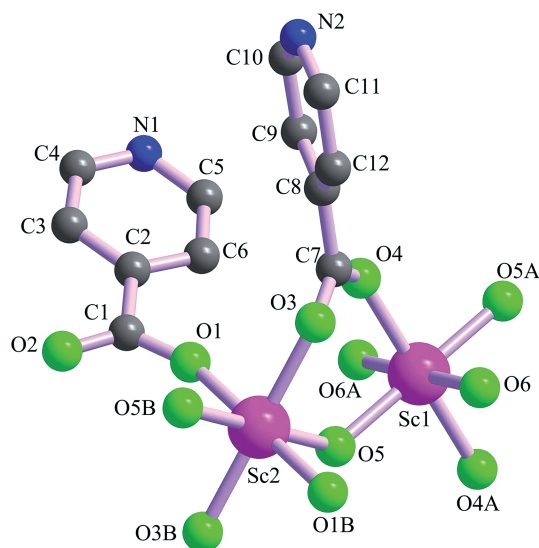
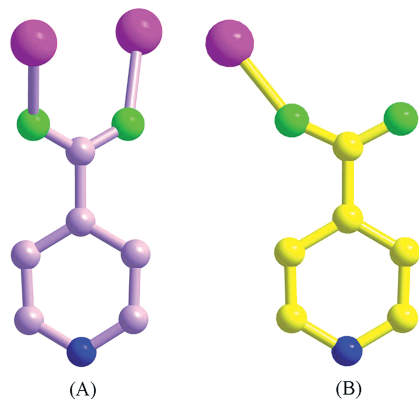


Figure 1. The coordination environment of the  $\text{Sc}^{\text{III}}$  ions in **1**. All hydrogen atoms are omitted for clarity. Symmetry codes: A,  $-x, 1-y, 2-z$ ; B,  $1-x, 1-y, 2-z$ .

The  $L^1$  ligand exhibits two distinct types of coordination modes, A and B, in **1** (Scheme 1). A (purple): two oxygen atoms of the carboxy group act in a monodentate mode, bridging two  $\text{Sc}^{\text{III}}$  centers; B (yellow): only one of the carboxy groups acts in a monodentate coordination mode,



Scheme 1. The two different coordination modes in **1** (Sc, pink; O, green; C, purple and yellow; N, blue).

whereas the other one remains uncoordinated. The nitrogen atom does not provide a coordinated site in **1**. The  $\text{ScO}_4$  units are linked to each other through OH groups, and this generates an infinite bent  $-\text{Sc}-\text{OH}-\text{Sc}-\text{OH}-$  chain with a Sc–OH–Sc angle of  $158^\circ$  (Figure 2a). As shown in Figure 2b, the  $-\text{Sc}-\text{OH}-\text{Sc}-\text{OH}-$  chains are linked by  $L^1$  ligands to form a new infinite 1D chain,  $\text{Sc}(\text{OH})(L^1)_2(\text{H}_2\text{O})$ . The plane-to-plane distances between the benzene rings of the  $L^1$  ligands in adjoining chains are about 3.3 Å. This suggests that contiguous chains are packed through strong  $\pi-\pi$  stacking interactions. The rings of the  $L^1$  ligand involved in the  $\pi-\pi$  stacking arrange in such a way that the six atoms of the ring do not completely overlap those of the

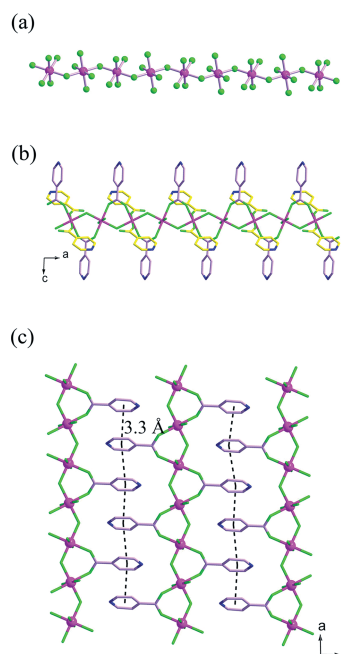


Figure 2. (a) The  $-\text{Sc}-\text{OH}-\text{Sc}-\text{OH}-$  chain in **1**. (b) The infinite 1D chain  $\text{Sc}(\text{OH})(L^1)_2(\text{H}_2\text{O})$ . (c) The  $\pi\cdots\pi$  interactions in **1**, in which  $L^1$  ligands of coordination mode B (yellow) were omitted (Sc, pink; O, green; C, purple and yellow; N, blue).

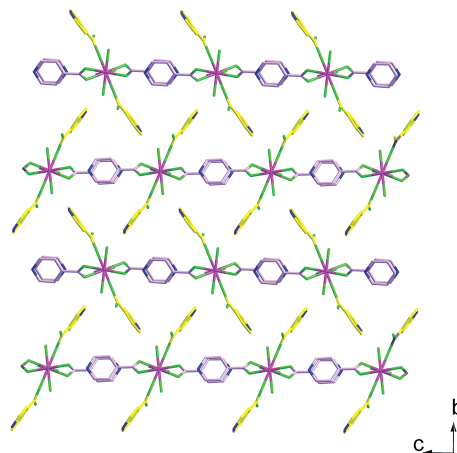


Figure 3. The packing diagram of **1** showing the projection along the  $bc$  direction. Hydrogen atoms are omitted for clarity (Sc, pink; O, green; C, purple and yellow; N, blue).

other rings. This means that the  $\pi$ - $\pi$  interaction is not “perfect face alignment” but “slipped stacking”. To more clearly describe the  $\pi$ - $\pi$  interactions in **1**,  $L^1$  ligands of coordination mode B (yellow) are omitted in Figure 2c. The packing diagrams of **1** display triangular windows showing the projection along the  $bc$  direction as depicted in Figure 3. This  $\pi$ - $\pi$  stacking plays an important role to stabilize the packing of such low-dimensional lattices. To the best of our knowledge, the -Sc-OH-Sc-OH- chain has rarely been reported in scandium coordination polymers.

## Crystal Structure of **2**

Compound **2** crystallizes in the orthorhombic space group *Fddd* and shows a 1D infinite chain. The asymmetric unit consists of three-quarters of a  $\text{Sc}^{\text{III}}$  ion, one  $L^2$  ligand, and one coordinated water molecule (Figure S2). As shown in Figure 4a, there are two types of  $\text{Sc}^{\text{III}}$  ions with different coordination environments. Sc1 is eight-coordinate, and its coordination geometry can be described as a triangular dodecahedron with four oxygen atoms and four nitrogen

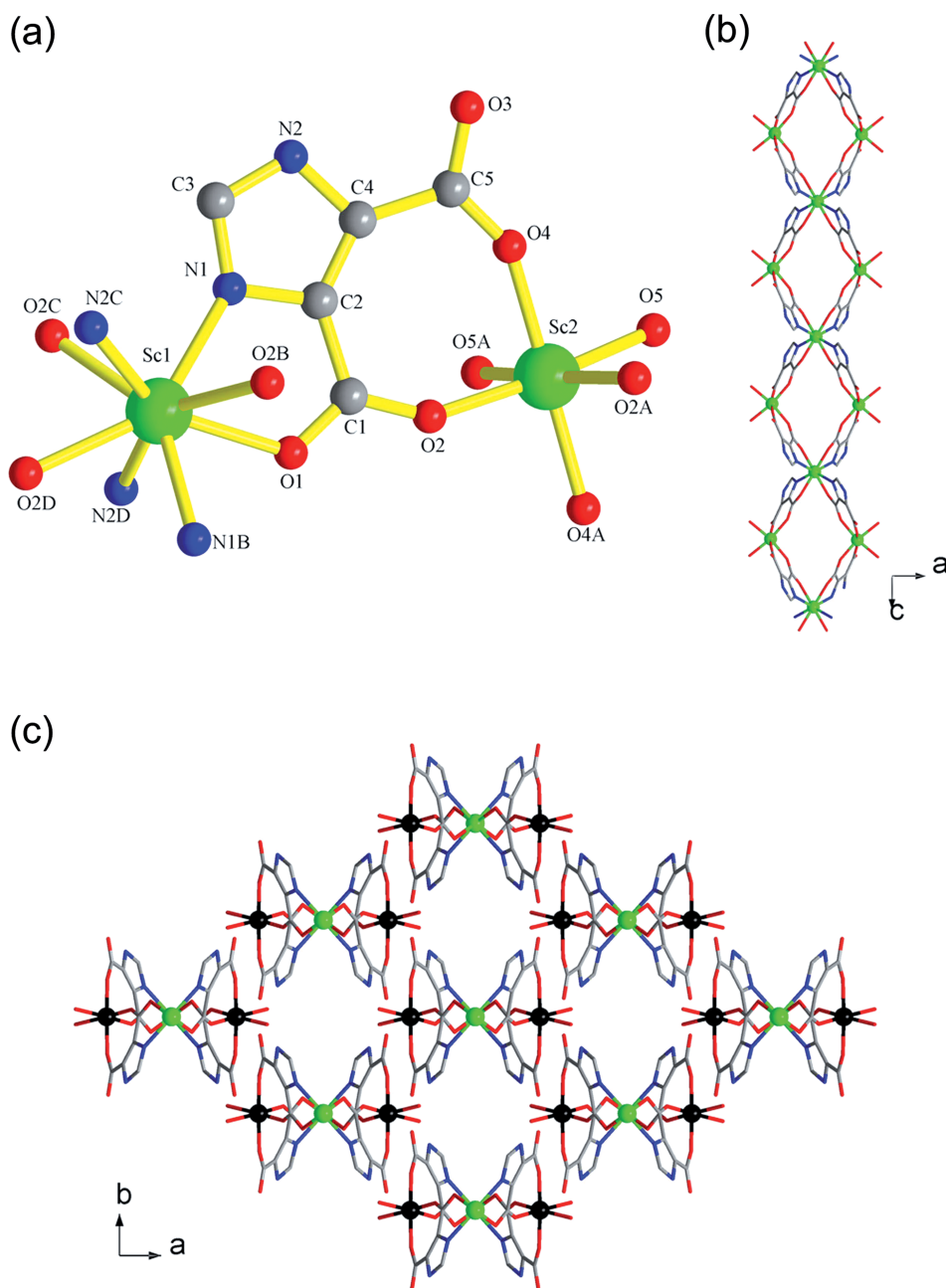


Figure 4. (a) The coordination environment of the  $\text{Sc}^{\text{III}}$  ions in **2**. (b) An infinite 1D chain along the  $ac$  direction. (c) The packing diagram of **2** showing the projection along the  $ab$  direction; black spheres are six-coordinate Sc2 ions, and green spheres are eight-coordinate Sc1 ions. Hydrogen atoms and guest molecules are omitted for clarity (Sc, black and green; O, red; C, dark gray; N, blue). Symmetry codes: A,  $-0.5 + x, 1.75 - y, 0.25 - z$ ; B,  $1.25 - x, 1.75 - y, -1.5 + z$ ; C,  $1 - 0.5 + x, 1.75 - y, -0.75 - z$ ; D,  $1.25 - x, y, 0.75 - z$ .

atoms from four different  $L^2$  ligands. Sc2 is six-coordinate, and its coordination geometry can be described as an octahedron with four monodentate carboxylate oxygen atoms from two independent  $L^2$  ligands, and two oxygen atoms from two OH groups to complete the coordination sphere. The Sc–O bond lengths fall in the region of 2.064(4)–2.262(4) Å and the Sc–N bond is 2.276(5) Å. These bond lengths are in agreement with those reported for other  $Sc^{III}$  compounds.<sup>[12]</sup> Sc1 and Sc2 are connected with  $L^2$  ligands to form an infinite 1D chain along the *ac* direction (Figure 4b). The 1D chain is butterfly-shaped and the neighboring chains are alternately stacked along the *ab* direction (Figure 4c). No intra- and interchain hydrogen bonds or  $\pi$ – $\pi$  stacking interactions were observed in **2**.

### Crystal Structure of **3**

Compound **3** crystallizes in the orthorhombic space group *Pbca*. The asymmetric unit consists of one  $Sc^{III}$  ion, one  $L^3$  ligand, one OH group, and two coordinated water molecules (Figure S3). As shown in Figure 5a, the  $Sc^{III}$  ion displays an octahedral geometry, being coordinated by two carboxylate oxygen atoms of one  $L^3$  ligand, two oxygen atoms from two OH groups, and two oxygen atoms from two coordinated water molecules. The Sc–O bond lengths

vary from 2.042(2) to 2.153(3) Å; these values are consistent with those of analogous compounds.<sup>[14]</sup> Sc1 and its corresponding centrosymmetrically generated atom Sc1A are joined by two  $\mu_2$ -O atoms of OH groups to give a binuclear unit of  $[Sc_2(OH)_2(L^3)_2(H_2O)_4]$  (Figure 5b), in which the distance between two Sc atoms is 3.1884(13) Å and the angle Sc1–O7–Sc1A is 78.16°. The packing diagram of compound **3** shows the projection along the *ac* direction as depicted in Figure 5c. No intra- and interchain hydrogen bonds or  $\pi$ – $\pi$  stacking interactions were observed in **3**.

### Thermogravimetric Analysis

Thermogravimetric analysis (TGA) was carried out at temperatures varying from 20 to 800 °C in air with a heating rate of 10 °C min<sup>−1</sup> (Figures S10–S12). As shown in Figure S10, compound **1** gradually loses lattice water from 80 to 300 °C, and then it decomposes rapidly. The weight loss of 78.48% (calcd. 78.72%) is in agreement with the decomposition of  $[Sc(OH)(L^1)_2(H_2O)]$  to  $ScO_{1.5}$ . Compound **2** displays a continuous weight loss of 77.31% (cal. 77.10%) in the temperature range 100–550 °C, which corresponds to the loss of guest molecules (nitrate anion and water molecule), coordinated water molecules, and  $L^2$  ligands. The remaining weight of 22.69% is attributed to the final product of  $Sc_2O_3$  (cal. 22.90%). The TGA plot of **3** also shows a continuing weight loss. The weight loss from 220 to 800 °C amounts to 72.50% (calcd. 72.75%), corresponding to the decomposition of  $[Sc_2(OH)_2(L^3)_2(H_2O)_4]$  to  $ScO_{1.5}$ .

### Catalytic Properties

The presence of unsaturated coordinated metal sites in solid materials is beneficial for catalytic reactions, providing Lewis acid sites in the structure. In the present work, there are unsaturated coordinated  $Sc^{III}$  ions (the six-coordinate  $Sc^{III}$  ions) in all of the compounds. Therefore, catalytic properties are expected for these compounds. To characterize the possible acid-type catalytic behavior of the unsaturated coordination in compounds **1–3**, the carbonyl cyanosilylation reaction was performed in the presence of all three compounds. The addition of  $CN^-$  to a carbonyl compound to form a cyanohydrin is one of the fundamental C–C bond formation reactions in organic chemistry.<sup>[13]</sup>

Compounds **1–3** were demonstrated to act as catalyst in the cyanosilylation reaction of aldehydes with trimethylsilyl cyanide (TMSCN) in  $CH_3CN$ . The reaction conditions were first established by using benzaldehyde as model substrate. The best conversion rate was obtained when 20% catalyst was used at room temperature. In order to further investigate the generality of the catalysts, we studied the influence of the different substituents of the aromatic aldehydes on the reaction under the same conditions. Kinetics results are shown in Figure 6, and the data are summarized in Table 1. Electron-withdrawing groups are known to improve the electropositivity of the carbon atom of the aro-

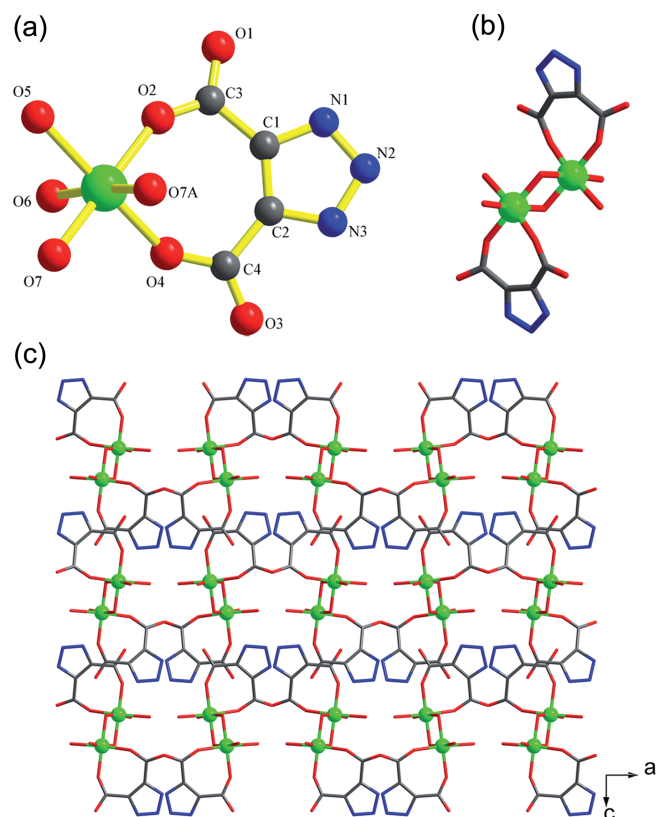


Figure 5. (a) The coordination environment of the  $Sc^{III}$  ions in **3**. (b) A binuclear unit of  $[Sc_2(OH)_2(L^3)_2(H_2O)_4]$  in **3**. (c) The packing diagram of **3** showing the projection along the *ac* direction. Hydrogen atoms are omitted for clarity (Sc, green; O, red; C, dark gray; N, blue). Symmetry codes: A,  $-x, -y, -z$ .



matic aldehyde, which favors the nucleophilic addition reaction between the aromatic aldehyde and TMSCN. Therefore, the conversion rate of the cyanosilylation reaction of *p*-nitrobenzaldehyde and TMSCN reaches 100% after 5 h

for **1**, and after 24 h for **2** and **3**. Moreover, the value of the conversion rate is in agreement with the electron-withdrawing ability of the substituent groups. For example, for **3**, the conversion rate decreases in the order *p*-nitrobenzaldehyde > *p*-bromobenzaldehyde > benzaldehyde > *p*-methoxybenzaldehyde > 1-naphthaldehyde. As shown in Figure 7, the catalytic activity of **1–3** for the cyanosilylation of aldehydes is rather high for *p*-nitrobenzaldehyde (100%, 5 h for **1** and 100%, 24 h for **2** and **3**). For the four remaining substrates, the order of the catalytic activity is **1** > **2** > **3** (Figure 7). This may correspond to the windows in the packing arrangement of **1** along the *bc* or *ab* directions (Figure 3 and Figure S13), and the six-coordinate Sc1 and Sc2 are exposed in this window. Compared to **3**, the free space surrounding the coordinated unsaturated metal sites (six-coordinate Sc2) in **2** is larger, which can provide a larger contact area for the reaction. Although the Sc<sup>III</sup> ion is also six-coordinate in **3**, probably geometrical constraints (Figure 5c and Figure S14) do not allow the reactants to diffuse inside the structure of the catalyst, and only the external surface area of this material becomes available for the reactants.

Table 1. Results for the cyanosilylation of carbonyl substrates in the presence of **1–3**.

$\text{Ar}-\text{C}(=\text{O})\text{H} + \text{Me}_3\text{SiCN} \xrightarrow[\text{CH}_3\text{CN}]{\text{Cat.}} \text{OSiMe}_3-\text{C}(\text{CN})(\text{H})\text{Ar}$			
Catalyst	Ar	Time (h)	Yield (%)
<b>1</b>	phenyl	20	100
	<i>p</i> -nitrophenyl	5	100
	<i>p</i> -bromophenyl	24	100
	<i>p</i> -methoxyphenyl	24	100
	1-naphthyl	24	74
<b>2</b>	phenyl	24	55
	<i>p</i> -nitrophenyl	8	98
	<i>p</i> -bromophenyl	24	42
	<i>p</i> -methoxyphenyl	24	37
	1-naphthyl	24	33
<b>3</b>	phenyl	24	25
	<i>p</i> -nitrophenyl	8	98
	<i>p</i> -bromophenyl	24	30
	<i>p</i> -methoxyphenyl	24	13
	1-naphthyl	24	6

After the reactions, the solid catalyst was recovered by centrifugation and washed with anhydrous acetonitrile and then characterized by powder X-ray diffraction (Figure S15). The powder diffraction patterns of the recovered catalysts are similar to those of the as-synthesized compounds. Reutilization is one of the greatest advantages of heterogeneous catalysts and can also provide useful information about the anchoring process and catalyst stability along the catalytic cycle. Recycling tests were carried out for all three compounds for the cyanosilylation of *p*-nitrobenzaldehyde. The catalyst was recycled after three runs. During the successive cycles, a small decrease in the activity was observed.

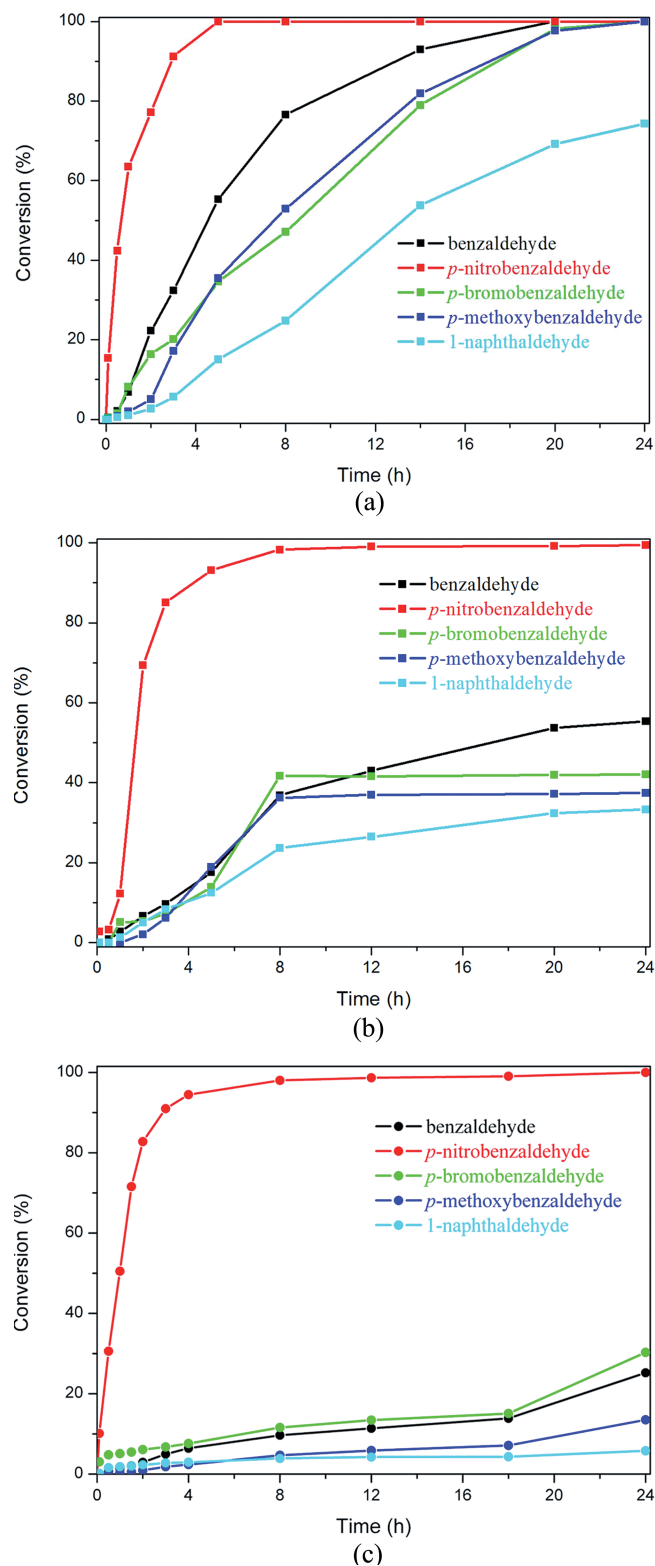


Figure 6. Plots of conversion vs. time for the cyanosilylation reaction with five different substrates for **1** (a), **2** (b), and **3** (c).

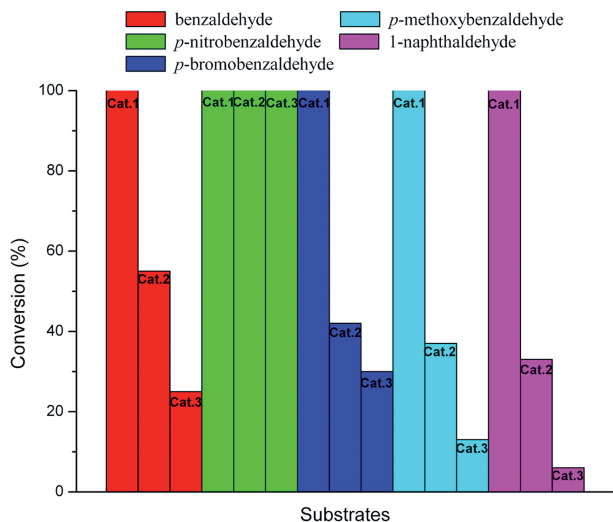


Figure 7. A comparison of conversion between catalysts **1**, **2**, and **3** (reaction time = 24 h).

As we know, the solvent has also a certain influence on catalyst activity. These three catalysts can maintain stability and activity in the presence of acetonitrile, dichloromethane, chloroform, tetrahydrofuran, or dioxane. When using acetonitrile as solvent, a better catalytic effect can be obtained. But when using tetrahydrofuran or dioxane as solvent, there are side reactions observed in the reaction system.

## Conclusions

In summary, three Sc compounds were prepared by using discrete carboxylate ligands under solvothermal conditions. These three new solid materials show high chemical stability in  $\text{CH}_3\text{CN}$ , as well as good Lewis acid catalytic ability for the cyanosilylation of aromatic aldehydes by virtue of their coordinative unsaturated metal sites. Moreover, they could be easily recovered by filtration and reused at least after three cycles without significant loss of yield. In addition, they also display intense fluorescence in the solid state at room temperature.

## Experimental Section

**General Procedures:** All the chemicals used in this work were of reagent grade and were used without purification. Powder X-ray diffraction (PXRD) data were collected with a Rigaku D/max-2550 diffractometer with  $\text{Cu-K}\alpha$  radiation ( $\lambda = 1.5418 \text{ \AA}$ ). Elemental analyses (C, H, and N) were performed with a Perkin–Elmer 2400 CHN Elemental Analyzer. IR spectra were recorded in the range  $400\text{--}4000 \text{ cm}^{-1}$  with a Nicolet Impact 410 spectrometer by using the KBr pellet method. Thermogravimetric analyses (TGA) were conducted with a Perkin–Elmer TGA 7 thermogravimetric analyzer by starting with ambient conditions and heating at a rate of  $10 \text{ }^\circ\text{C min}^{-1}$  from room temperature to  $800 \text{ }^\circ\text{C}$ . Photoluminescence

(PL) spectra were measured with an Edinburgh Instruments FLS920 spectrophotometer.  $^1\text{H}$  NMR spectra were measured with a Bruker Avance 400 console at a frequency of 400 MHz.

**Compound 1:**  $\text{Sc}(\text{NO}_3)_3 \cdot 6\text{H}_2\text{O}$  (0.2 mmol in 2.5 mL  $\text{H}_2\text{O}$ ) and isonicotinic acid (0.0369 g, 0.3 mmol) were dispersed in water (5 mL) in a 20 mL glass jar with a lid and heated at  $80 \text{ }^\circ\text{C}$  for 16 h. The mixture was then cooled to room temperature under ambient conditions. Colorless block crystals of **1** were recovered by filtration, washed with distilled water, and dried in air. The yield of the product was 82% in weight percent based on Sc.  $\text{C}_{12}\text{H}_{11}\text{N}_2\text{O}_6\text{Sc}$  (324): calcd. C 44.46, H 3.42, N 8.64; found C 44.25, H 3.61, N 8.49. Selected IR data (KBr pellet):  $\tilde{\nu} = 3442$  (s), 3000 (s), 2368 (w), 1554 (s), 1385 (s), 1158 (w), 1021 (m), 761 (m), 669 (m),  $458 \text{ cm}^{-1}$ .

**Compound 2:**  $\text{Sc}(\text{NO}_3)_3 \cdot 6\text{H}_2\text{O}$  (0.2 mmol in 2.5 mL  $\text{H}_2\text{O}$ ) and 4,5-imidazole dicarboxylic acid (0.0624 g, 0.4 mmol) were dispersed in acetonitrile (5 mL) and concentrated hydrochloric acid (0.05 mL) in a 23 mL Teflon-lined autoclave. The mixture was heated under autogenous pressure at  $105 \text{ }^\circ\text{C}$  for 3 d and then cooled to room temperature under ambient conditions. Yellow block crystals of **2** were recovered by filtration, washed with distilled water, and dried in air. The yield of product was 82% in weight percent based on Sc.  $\text{C}_{20}\text{H}_{18}\text{N}_9\text{O}_{24}\text{Sc}_3$  (903): calcd. C 26.59, H 2.01, N 13.96; found C 26.25, H 2.07, N 13.64. Selected IR data (KBr pellet):  $\tilde{\nu} = 3442$  (s), 3149 (s), 1572 (s), 1500 (w), 1408 (m), 1242 (m), 1120 (m), 980 (w), 841 (m), 648 (m),  $523 \text{ cm}^{-1}$ .

**Compound 3:**  $\text{Sc}(\text{NO}_3)_3 \cdot 6\text{H}_2\text{O}$  (0.2 mmol in 2.5 mL  $\text{H}_2\text{O}$ ) and 1,2,3-triazole-4,5-dicarboxylic acid (0.0393 g, 0.25 mmol) were dispersed in  $\text{CH}_3\text{CN}$  (8 mL) and NaOH (1 M, 0.3 mL) in a 23 mL Teflon-lined autoclave and heated under autogenous pressure at  $120 \text{ }^\circ\text{C}$  for 3 d. The mixture was then cooled to room temperature under ambient conditions. Yellow block crystals of **3** were recovered by filtration, washed with distilled water, and dried in air. The yield of product was 85% in weight percent based on Sc.  $\text{C}_8\text{H}_{12}\text{N}_6\text{O}_{14}\text{Sc}_2$  (506): calcd. C 18.98, H 2.39, N 16.60; found C 19.75, H 2.41, N 16.64. Selected IR data (KBr pellet):  $\tilde{\nu} = 3394$  (s), 1624 (s), 1478 (w), 1357 (m), 1393 (m), 1131 (w), 981 (w), 838 (m), 616 (w),  $510 \text{ cm}^{-1}$ .

**Single-Crystal X-ray Structure Determination:** Suitable single crystals of **1–3** were selected for single-crystal X-ray diffraction analysis. The intensity data collection was performed with a Rigaku R-Axis RAPID diffractometer equipped with graphite-monochromated  $\text{Mo-K}\alpha$  ( $\lambda = 0.71073 \text{ \AA}$ ) radiation in the  $\omega$  scanning mode at room temperature. No significant decay was observed during the data collection. Data processing was accomplished with the RAPID AUTO processing program. The structures were solved by direct methods and refined by full-matrix least-squares on  $F^2$  by using the SHELXTL crystallographic software package.<sup>[14]</sup> All the non-hydrogen atoms were refined anisotropically. All the hydrogen atoms attached to carbon atoms were placed geometrically and located theoretically on the basis of a riding model. The unit cell volume of **2** includes a large region of disordered nitrate anion and water molecule, which could not be modeled as discrete atomic sites. We employed PLATON/SQUEEZE<sup>[15]</sup> to calculate the contribution to the diffraction from the solvent region. The final formula was calculated from the SQUEEZE results combined with elemental analysis data and TGA data.<sup>[16]</sup> Experimental details for the structural determinations of **1–3** are summarized in Table 2, while selected bond lengths and angles are presented in Tables S1–S3. CCDC-980253 (for **1**), -978974 (for **2**), and -978973 (for **3**) contain the supplementary crystallographic data for this paper. These data can be obtained free of charge from The Cambridge Crystallographic Data Centre via [www.ccdc.cam.ac.uk/data\\_request/cif](http://www.ccdc.cam.ac.uk/data_request/cif).

Table 2. Crystal and structure refinement details for 1–3.

Compound	1	2	3
Formula	C <sub>12</sub> H <sub>11</sub> O <sub>6</sub> N <sub>2</sub> ScC <sub>20</sub> H <sub>18</sub> O <sub>24</sub> N <sub>9</sub> Sc <sub>3</sub> C <sub>8</sub> H <sub>12</sub> O <sub>14</sub> N <sub>6</sub> Sc <sub>2</sub>		
Formula weight	324	903	506
T (K)	293(2)	293(2)	293(2)
Crystal system	monoclinic	orthorhombic	orthorhombic
Space group	P2 <sub>1</sub> /C	Fddd	Pbca
a (Å)	7.4582(15)	31.8861(12)	14.121(3)
b (Å)	18.454(4)	20.2788(6)	6.7919(14)
c (Å)	10.380(2)	10.5793(3)	17.397(3)
α (°)	90	90	90
β (°)	92.01(3)	90	90
γ (°)	90	90	90
V (Å <sup>3</sup> )	6840.7(4)	6840.7(4)	1668.5(6)
Z	4	8	4
D <sub>c</sub> (g/cm <sup>3</sup> )	1.494	1.567	1.975
F(000)	652.0	3256.0	976
μ (mm <sup>−1</sup> )	0.543	0.669	0.908
R <sub>int</sub>	0.0648	0.0472	0.0979
GOF	1.071	1.092	1.039
R <sub>1</sub> , wR <sub>2</sub>	0.0469, 0.0953,	0.0481,	
[I > 2σ(I)] <sup>[a,b]</sup>	0.1341	0.2189	0.1238
R <sub>1</sub> , wR <sub>2</sub>	0.0689, 0.0988,	0.0700,	
(all data) <sup>[a,b]</sup>	0.1465	0.2202	0.1351

[a]  $R_1 = \Sigma |F_o| - |F_c| / \Sigma |F_o|$ . [b]  $wR_2 = \Sigma [w(F_o^2 - F_c^2)^2] / \Sigma [w(F_o^2)^2]^{1/2}$ .

**Catalytic Experiment:** The catalysts were soaked in MeOH for 24 h, and then heated under vacuum at 85 °C for 16 h. A typical cyano-silylation procedure was performed as follows: activated catalyst (0.1 mmol) was suspended in dry acetonitrile (5 mL) followed by the addition of the aldehyde (0.5 mmol) and trimethylsilyl cyanide (1.2 mmol). The reaction mixtures were stirred at room temperature. The yields of the reactions were determined by <sup>1</sup>H NMR spectroscopy and were calculated on the basis of the carbonyl substrate. Catalytic recyclability was checked for three times with the same batch of catalyst, and no obvious decrease in activity was observed. The observed yields in three consecutive runs were 100%, 98%, and 99% for 1, 100%, 97%, and 98% for 2, and 100%, 96%, and 97% for 3.

## Acknowledgments

We gratefully acknowledge the financial support of the National Natural Science Foundation of China (Nos. 21171065, 21201077).

- P. M. Forster, A. K. Cheetham, *Top. Catal.* **2003**, *24*, 79–86.
- a) R. K. Das, A. Aijaz, M. K. Sharma, P. Lama, P. K. Bharadwaj, *Chem. Eur. J.* **2012**, *18*, 6866–6872; b) A. Corma, H. Garcia, F. X. L. Xamena, *Chem. Rev.* **2010**, *110*, 4606–4655; c) A. M. Shultz, O. K. Farha, J. T. Hupp, S. T. Nguyen, *J. Am. Chem. Soc.* **2009**, *131*, 4204–4205; d) J. S. Seo, D. Whang, H. Lee, S. I. Jun, J. Oh, Y. J. Jeon, K. Kim, *Nature* **2000**, *404*, 982–986; e) C. D. Wu, A. Hu, L. Zhang, W. Lin, *J. Am. Chem. Soc.* **2005**, *127*, 8940–8941; f) T. Uemura, R. Kitaura, Y. Ohta, M. Nagaoka, S. Kitagawa, *Angew. Chem.* **2006**, *118*, 4218–4222; g) T. Uemura, R. Kitaura, Y. Ohta, M. Nagaoka, S. Kitagawa, *Angew. Chem. Int. Ed.* **2006**, *45*, 4112–4116; *Angew. Chem.* **2006**, *118*, 4218; h) L. Ma, J. M. Falkowski, C. Abney, W. Lin, *Nat. Chem.* **2010**, *2*, 838–846; i) K. Gedrich, M. Heitbaum, A. Notzon, I. Senkovska, R. Froehlich, J. Getzschmann, U. Mueller, F. Glorius, S. Kaskel, *Chem. Eur. J.* **2011**, *17*, 2099–2103.
- a) L. Ma, C. Abney, W. Lin, *Chem. Soc. Rev.* **2009**, *38*, 1248–1256; b) X. M. Lin, T. T. Li, Y. W. Wang, L. Zhang, C. Y. Su, *Chem. Asian J.* **2012**, *7*, 2796–2804; c) L. Ma, W. Lin, *Top. Curr. Chem.* **2010**, *293*, 175–205; d) M. Ranocchiari, J. A. van Bokhoven, *Phys. Chem. Chem. Phys.* **2011**, *13*, 6388–6396; e) D. Farrusseng, S. Aguado, C. Pinel, *Angew. Chem.* **2009**, *121*, 7638–7649; f) D. Farrusseng, S. Aguado, C. Pinel, *Angew. Chem. Int. Ed.* **2009**, *48*, 7502–7513; *Angew. Chem.* **2009**, *121*, 7638; g) Y. Huang, Z. Zheng, T. Liu, J. Lü, Z. Lin, H. Li, R. Cao, *Catal. Commun.* **2011**, *14*, 27–31; h) Y. Huang, S. Liu, Z. Lin, W. Li, X. Li, R. Cao, *J. Catal.* **2012**, *292*, 111–117; i) Y. Huang, Z. Lin, R. Cao, *Chem. Eur. J.* **2011**, *17*, 12706–12712; j) J. Y. Lee, O. K. Farha, J. Roberts, K. A. Scheidt, S. B. T. Nguyen, J. T. Hupp, *Chem. Soc. Rev.* **2009**, *38*, 1450–1459; k) Y. Huang, T. Liu, J. Lin, J. Lü, Z. Lin, R. Cao, *Inorg. Chem.* **2011**, *50*, 2191–2198; l) A. Dhakshinamoorthy, H. Garcia, *Chem. Soc. Rev.* **2012**, *41*, 5262–5284; m) K. Kim, M. Banerjee, M. Yoon, S. Das, *Top. Curr. Chem.* **2010**, *293*, 115–153; n) M. Yoon, R. Srirambalaji, K. Kim, *Chem. Rev.* **2012**, *112*, 1196–1231.
- a) S. Nagayama, S. Kobayashi, *Angew. Chem. Int. Ed.* **2000**, *39*, 567–569; *Angew. Chem.* **2000**, *112*, 578; b) B. Karimi, L. Ma'Mani, *Org. Lett.* **2004**, *6*, 4813–4815.
- F. Gándara, B. Gómez-Lor, M. Iglesias, N. Snejko, E. Gutiérrez-Puebla, A. Monge, *Chem. Commun.* **2009**, 2393–2395.
- J. Perles, M. Iglesias, C. Ruiz-Valero, N. Snejko, *Chem. Commun.* **2003**, 346–347.
- a) S. Kobayashi, M. Sugiura, H. Kitagawa, W. W. L. Lam, *Chem. Rev.* **2002**, *102*, 2227–2302; b) B. Karimi, L. Ma'mani, *Tetrahedron Lett.* **2003**, *44*, 6051–6053.
- a) J. Perles, M. Iglesias, C. Ruiz-Valero, N. Snejko, *Chem. Commun.* **2003**, 346–347; b) J. Perles, M. Iglesias, M. A. Martín-Luengo, M. A. Monge, C. Ruiz-Valero, N. Snejko, *Chem. Mater.* **2005**, *17*, 5837–5842; c) P. D. C. Dietzel, R. Blom, H. Fjellvag, *Dalton Trans.* **2006**, 2055–2057.
- a) L. F. Tietze, U. Beifuss, *Comprehensive Organic Synthesis* Pergamon, New York, **1991**, p. 341; b) H. Pines, M. Stalick, *Base-Catalyzed Reactions of Hydrocarbons and Related Compounds*, Academic Press, New York **1977**, p. 234.
- a) R. J. H. Gregory, *Chem. Rev.* **1999**, *99*, 3649; b) M. North, *Tetrahedron: Asymmetry* **2003**, *14*, 147–176.
- a) O. Ohmori, M. Fujita, *Chem. Commun.* **2004**, 1586–1587; b) S. Horike, M. Dincă, K. Tamaki, J. R. Long, *J. Am. Chem. Soc.* **2008**, *130*, 5854–5855; c) S. Hasegawa, S. Horike, R. Matsuda, S. Furukawa, K. Mochizuki, Y. Kinoshita, S. Kitagawa, *J. Am. Chem. Soc.* **2007**, *129*, 2607–2614; d) D. Y. Hong, K. H. Young, C. Serre, G. Frey, J. S. Chang, *Adv. Funct. Mater.* **2009**, *19*, 1537–1552.
- a) I. A. Ibarra, S. H. Yang, X. Lin, A. J. Blake, P. J. Rizkallah, H. Nowell, D. R. Allan, N. R. Champness, P. Hubberstey, M. Schröder, *Chem. Commun.* **2011**, *47*, 8304–8306; b) I. A. Ibarra, X. Lin, S. H. Yang, A. J. Blake, G. S. Walker, S. A. Barnett, D. R. Allan, N. R. Champness, P. Hubberstey, M. Schröder, *Chem. Eur. J.* **2010**, *16*, 13671–13679; c) J. Perles, N. Snejko, M. Iglesias, M. A. Monge, *J. Mater. Chem.* **2009**, *19*, 6504–6511; d) S. R. Miller, P. A. Wright, T. Devic, C. Serre, G. Férey, P. L. Llewellyn, R. Denoyel, L. Gaberova, Y. Filinchuk, *Langmuir* **2009**, *25*, 3618–3626; e) S. A. Cotton, V. M. A. Fisher, P. R. Raithby, S. Schiffrs, S. J. Teat, *Inorg. Chem. Commun.* **2008**, *11*, 822–824; f) S. R. Miller, P. A. Wright, C. Serre, T. Loiseau, J. Marroth, G. Férey, *Chem. Commun.* **2005**, 3850–3852; g) M. A. Katkova, V. A. Ilichev, G. K. Fukin, M. N. Bochkarev, *Inorg. Chim. Acta* **2009**, *362*, 1393–1395.
- a) M. Fujita, Y. J. Kwon, S. Washizu, K. Ogura, *J. Am. Chem. Soc.* **1994**, *116*, 1151–1152; b) A. Henschel, K. Gedrich, R. Kraehnert, S. Kaskel, *Chem. Commun.* **2008**, 4192–4194; c) P. Phuengphai, S. Youngme, P. Gamez, J. Reedijk, *Dalton Trans.* **2010**, *39*, 7936–7942; d) T. Ladrak, S. Smulders, O. Roubeau, S. J. Teat, P. Gamez, J. Reedijk, *Eur. J. Inorg. Chem.* **2010**, 3804–3812; e) D. Dang, P. Wu, C. He, Z. Xie, C. Duan, *J. Am. Chem. Soc.* **2010**, *132*, 14321–14323; f) S. Nayak, K. Harms, S. Dehnen, *Inorg. Chem.* **2011**, *50*, 2714–2716.

- [14] a) G. M. Sheldrick, *SHELXTL-NT*, Version 5.1, Bruker AXS Inc., Madison, WI, **1997**; b) D. T. Cromer, J. T. Waber, *International Tables for X-ray Crystallography, Vol. 4*, Kynoch Press, Birmingham, AL, **1974** (Table 2, 2A).
- [15] a) G. R. Desiraju, *Acc. Chem. Res.* **1996**, *29*, 441–449; b) T. Steiner, *Angew. Chem. Int. Ed.* **2002**, *41*, 48–76; *Angew. Chem.* **2002**, *114*, 50; c) G. A. Jeffrey, *An Introduction to Hydrogen Bonding*, Oxford University Press, New York, **1997**.
- [16] a) I. A. Ibarra, X. Lin, S. H. Yang, A. J. Blake, G. S. Walker, S. A. Barnett, D. R. Allan, N. R. Champness, P. Hubberstey, M. Schröder, *Chem. Eur. J.* **2010**, *16*, 13671–13679; b) P. D. C. Dietzel, R. Blom, H. Fjellvåg, *Dalton Trans.* **2006**, 2055–2057.

Received: August 1, 2014

Published Online: January 22, 2015